

1 **Title:** Microbiome-TP53 Gene Interaction in Human Lung Cancer

2 **Running Title:** Microbiome-Gene Interaction in Lung Cancer

3 **Authors:** K. Leigh Greathouse<sup>1†</sup>, James R. White<sup>2</sup>, Ashely J. Vargas<sup>1</sup>, Valery V.

4 Bliskovsky<sup>3</sup>, Jessica A. Beck<sup>1</sup>, Natalia von Muhlinen<sup>1</sup>, Eric C. Polley<sup>4</sup>, Elise D.

5 Bowman<sup>1</sup>, Mohammed A. Khan<sup>1</sup>, Ana I. Robles<sup>1</sup>, Tomer Cooks<sup>1</sup>, Brid M. Ryan<sup>1</sup>, Amiran

6 H. Dzutsev<sup>5</sup>, Giorgio Trinchieri<sup>5</sup>, Marbin A. Pineda<sup>6</sup>, Sven Bilke<sup>6</sup>, Paul S. Meltzer<sup>6</sup>, Alexis

7 N. Hokenstad<sup>7</sup>, Tricia M. Stickrod<sup>8</sup>, Marina R. Walther-Antonio<sup>7,9</sup>, Joshua P. Earl<sup>10</sup>,

8 Joshua C. Mell<sup>10</sup>, Jaroslaw E. Krol<sup>10</sup>, Sergey V. Balashov<sup>10</sup>, Archana S. Bhat<sup>10</sup>, Garth D.

9 Ehrlich<sup>10</sup>, Alex Valm<sup>11</sup>, Clayton Deming<sup>11</sup>, Sean Conlan<sup>11</sup>, Julia Oh<sup>12</sup>, Julie A. Segre<sup>11</sup>,

10 Curtis C. Harris<sup>1\*</sup>

11 **Author Affiliations:** <sup>1</sup>Laboratory of Human Carcinogenesis, Center for Cancer

12 Research, National Cancer Institute, National Institutes of Health, Bethesda, MD,

13 20892, <sup>2</sup>Resphera Biosciences, Baltimore, MD, 21231, <sup>3</sup>Center for Cancer Research

14 Genomics Core, National Cancer Institute, National Institutes of Health, Bethesda, MD,

15 20892, <sup>4</sup>Division of Biomedical Statistics and Informatics, Mayo Clinic, Rochester, MN,

16 55905, <sup>5</sup>Laboratory of Experimental Immunology, Center for Cancer Research, National

17 Cancer Institute, National Institutes of Health, Bethesda, MD, 20892, <sup>6</sup>Genetics Branch,

18 Center for Cancer Research, National Cancer Institute, National Institutes of Health

19 Bethesda, MD, 20892, <sup>7</sup>Department of Obstetrics and Gynecology, Mayo Clinic,

20 Rochester, MN, <sup>8</sup>Microbiome Laboratory, Mayo Clinic, Rochester, MN, 55905,

21 <sup>9</sup>Department of Surgery, Mayo Clinic, Rochester, MN, 55905, <sup>10</sup>Department of

22 Microbiology and Immunology and Center for Genomic Sciences, Institute of Molecular

23 Medicine and Infectious Disease, Drexel University College of Medicine, Philadelphia,

1 PA, 19129, <sup>11</sup>National Human Genome Research Institute, National Institutes of Health,  
2 Bethesda, MD, 20892, <sup>12</sup>Jackson Laboratory, Framingham, CT, 06032.\*Corresponding  
3 author, <sup>†</sup> Currently, Nutrition Sciences, Baylor University, Waco, TX, 97346.

4 **Corresponding Author:** Curtis C Harris, M.D.

5 Laboratory of Human Carcinogenesis

6 National Cancer Institute

7 37 Convent Dr., Rm 3068A, MSC 4258

8 Bethesda, MD. 20892-4258

9 Phone: 301-496-2048

10 Fax: 301-496-0497

11 Email: [curtis\\_harris@nih.gov](mailto:curtis_harris@nih.gov)

12

13 **Keywords: Lung Cancer, Microbiome, TP53, Squamous Cell Carcinoma, Mutation**

14

15

16

17

18

19

20

21

22

23

1 **Abstract:**

2 **Background:** Lung cancer is the leading cancer diagnosis worldwide and the number  
3 one cause of cancer deaths. Exposure to cigarette smoke, the primary risk factor in lung  
4 cancer, reduces epithelial barrier integrity and increases susceptibility to infections.  
5 Herein, we hypothesized that somatic mutations together with cigarette smoke generate  
6 a dysbiotic microbiota that is associated with lung carcinogenesis. Using lung tissue  
7 from controls (n=33) and cancer cases (n=143), we conducted 16S rRNA bacterial gene  
8 sequencing, with RNA-seq data from lung cancer cases in The Cancer Genome Atlas  
9 (n=1112) serving as the validation cohort.

10 **Results:** Overall, we demonstrate a lower alpha diversity in normal lung as compared to  
11 non-tumor adjacent or tumor tissue. In squamous cell carcinoma (SCC) specifically, a  
12 separate group of taxa were identified, in which *Acidovorax* was enriched in smokers ( $P$   
13 =0.0013). *Acidovorax temporans* was identified by fluorescent *in situ* hybridization within  
14 tumor sections, and confirmed by two separate 16S rRNA strategies. Further, these  
15 taxa, including *Acidovorax*, exhibited higher abundance among the subset of SCC  
16 cases with *TP53* mutations, an association not seen in adenocarcinomas (AD).

17 **Conclusions:** The results of this comprehensive study show both a microbiome-gene  
18 and microbiome-exposure interactions in SCC lung cancer tissue. Specifically, tumors  
19 harboring *TP53* mutations, which can damage epithelial function, have a unique  
20 bacterial consortia which is higher in relative abundance in smoking-associated SCC.  
21 Given the significant need for clinical diagnostic tools in lung cancer, this study may  
22 provide novel biomarkers for early detection.

23

1

2 **Background:** Lung cancer is the leading cancer diagnosis worldwide (1.8 million/year)  
3 and has a higher mortality than that of the next top three cancers combined (158,080 vs  
4 115,760 deaths) [1]. Unfortunately, lung cancer survival remains poor and has shown  
5 minimal improvement over the past five decades, owing to diagnosis at advanced stage  
6 and resistance to standard chemotherapy [2]. While we have made significant strides with  
7 targeted receptor therapy and immunotherapy, biomarkers with higher specificity would  
8 improve diagnosis and treatment for these individuals.

9 Epidemiological evidence indicates an association between repeated antibiotic exposure  
10 and increased lung cancer risk, however, the contribution of the lung microbiome to lung  
11 cancer is unknown [3]. The first line of defense against inhaled environmental insults,  
12 including tobacco smoke and infection, is the respiratory epithelium. Until recently,  
13 healthy lungs were regarded as essentially sterile; however, studies now illustrate the  
14 presence of a lung microbiota [4], the community of microscopic organisms living within  
15 the host lung, which is altered in respiratory diseases including asthma, chronic  
16 obstructive pulmonary disease (COPD) and cystic fibrosis [5]. Disruption of the epithelium  
17 by tobacco smoke can be a primary cause of inflammatory pathology, which is seen in  
18 both COPD and lung cancer. Dysbiosis has been observed in both humans and model  
19 systems of COPD and cystic fibrosis [6, 7]. In COPD patients and *in vitro*, cigarette smoke  
20 has been shown to reduce epithelial integrity and cell-cell contact, which can increase  
21 susceptibility to respiratory pathogens or other environmental pollutants [8]. Disturbances  
22 in the microbiome, from cigarette smoke, epithelial damage or gene mutations, can allow  
23 pathogenic species to dominate the community or increase virulence of other normally

1 commensal microbes. Evidence of this has been demonstrated in patients with cystic  
2 fibrosis who have more virulent forms of *P. aeruginosa* [9]. These inflammatory  
3 associated events have been proposed to lead to an increased risk or progression of  
4 diseases, including lung cancer.

5 Several bacteria are associated with chronic inflammation and subsequent increased risk  
6 of lung and colon cancer, including *Mycobacterium tuberculosis* (lung cancer) [10]  
7 *Bacteroides fragilis* and *Fusobacterium nucleatum* (colon cancer) [11]. Recent  
8 microbiome studies in colon cancer have demonstrated a contribution of bacteria to  
9 carcinogenesis. Specifically, *F. nucleatum*, a bacterium commonly isolated from patients  
10 with inflammatory bowel disease, may be a risk factor for colon cancer [11, 12]. The more  
11 virulent strains of *F. nucleatum* affect colon cancer progression in animal models and  
12 increase tumor multiplicity [13] by various mechanisms including favoring the infiltration  
13 of tumor-promoting myeloid cells to create a pro-inflammatory environment [14].  
14 Colorectal carcinomas associated with high abundance of fecal *F. nucleatum* were found  
15 to have the highest number of somatic mutations, suggesting that these mutations create  
16 a pathogen-friendly environment [15]. Similarly, *B. fragilis* can secrete endotoxins that  
17 cause DNA damage leading to mutations and colon cancer initiation [16]. Furthermore,  
18 the loss of the oncogenic protein p53 in enterocytes impairs the epithelial barrier and  
19 allows infiltration of bacteria resulting in inflammatory signaling (NF- $\kappa$ B), which is required  
20 for tumor progression [17]. The tumor suppressor gene *TP53* is the most commonly  
21 mutated gene in lung cancer [18], with certain missense mutations showing gain of  
22 oncogenic function [19]; however, the relationship between *TP53* and microbiota in lung  
23 cancer remains unknown. Herein, we hypothesize that somatic mutations together with

1 alterations in the lung microbiome create an inflammatory environment, which participate  
2 in lung carcinogenesis.

### 3 **Results:**

4 To investigate the lung mucosal-associated microbial alterations in the etiology of lung  
5 cancer, we analyzed samples from the NCI-MD case-control study (n=143 tumor and  
6 n=144 non-tumor adjacent tissues) and lung cancer samples from The Cancer Genome  
7 Atlas (n=1112 tumor and non-tumor adjacent RNA-seq data from tissues) for validation.  
8 In addition, we used the clinical information from these two sample populations to control  
9 for confounders in lung cancer risk and progression (age, gender, smoking, race, family  
10 and medical history and co-morbidities), as well as factors that are known to alter the  
11 human microbiome (antibiotics and neo-adjuvant therapy). Given the paucity of healthy  
12 lung tissue available for study, we utilized two separate tissue biorepositories. Non-  
13 cancerous lung tissue was obtained by lung biopsy from individuals with benign lung  
14 nodules without cancer or non-cancer lung from immediate autopsy [20], which was used  
15 as a referent control (see Additional file 1: Table 1). Given the high potential for  
16 contamination in low-biomass samples, such as the lung, we took several measures to  
17 address this issue controlling for contamination points in the collection process. In order  
18 to remove possible contaminants from our analysis, we first performed a threshold  
19 analysis similar to a previous study [21], wherein we plotted the mean percent abundance  
20 across experimental samples versus negative control samples and removed those that  
21 were  $\geq 5\%$  in both experimental and negative control samples (see Additional file 1: Figure  
22 S1). Additionally, we conducted hierarchal clustering of negative controls, non-tumor and  
23 tumor samples independently in order to visualize and identify the strongest sources of

1 contamination (see Additional file 1: Figure S2). The combination of these analyses  
2 resulted in initial removal of the genera *Halomonas*, *Herbaspirillum*, *Shewanella*,  
3 *Propionibacterium* and *Variovorax*.

4 To identify the microbial communities present in each tissue type, we sequenced the V3-  
5 5 16S rRNA bacterial gene using the Illumina MiSeq platform. After quality filtering and  
6 contaminant removal, 34 million quality sequences were retained for OTU clustering and  
7 downstream analysis (see Additional file 1: Table 2).

8 To enable us to validate findings from our NCI-MD 16S rRNA gene sequencing analysis  
9 we took advantage of the TCGA lung cancer database. Using the unmapped RNA-seq  
10 reads from these samples (N=1112 and n=106 paired tumor/non-tumor), we analyzed  
11 with our metagenomics analysis pipeline. After removal of all human reads, we took the  
12 remaining non-human reads and used three separate tools, MetaPhlAn, Kraken and  
13 PathoScope, to assign reads to taxonomy, including bacteria, virus, and fungi. Due to the  
14 highly curated database of PathoScope, we were able obtain to species and in some  
15 cases strain-level putative identification of RNA-seq reads. For this reason, and due to its  
16 rigorous validation in other studies [22], we used these data as our validation data set.  
17 Unfortunately, given that all patients in this database had lung cancer, we could not  
18 validate our microbial findings in non-diseased lung tissue in the TCGA data set. Given  
19 that this was one of the first times TCGA was used to completely profile the microbiota of  
20 lung cancer, we asked how similar the 16S rRNA gene sequencing and RNA-seq  
21 microbial communities were at the phylum and genus levels. Using an overall threshold  
22 of 0.01% of genus level abundance, we identified 236 overlapping genera out of 520 total

1 genera in the 16S rRNA gene sequencing data and 609 total genera in the RNA-seq data  
2 (see Additional file 1: Figure S3).

3 **Bacterial profile of the lung cancer microbiome is dominated by Proteobacteria and**  
4 **validated in a separate lung cancer data set.** We know from previous microbial studies  
5 of lung disease that bacterial composition shifts occur compared to normal non-diseased  
6 lungs [23] and associated with disease severity [24], however these compositional  
7 changes have not been examined in lung cancer. In order to identify the microbial  
8 changes associated with lung cancer, we first examined the ecological diversity within  
9 samples (alpha diversity) and between samples (beta diversity) of non-cancerous  
10 (immediate autopsy and hospital biopsy) tissues, non-tumor adjacent (NT) and tumor (T)  
11 tissues from 16S rRNA gene sequencing. At the phylum level, we observed increases in  
12 Proteobacteria (Kruskal-Wallis  $P=0.0002$ ) and decreases in Firmicutes (Kruskal-Wallis  
13  $P=0.04$ ) in lung tissue hospital biopsies, as well as, in tumor and associated non-tumor  
14 tissues from the NCI-MD study compared with non-cancer population control lung tissues,  
15 as has been seen in COPD[25] (Figure 1A). We also observed a similar increase in  
16 Proteobacteria (Mann-Whitney  $P=0.02$ ) between non-tumor lung tissue and lung cancer  
17 in the TCGA study, indicating that this is recurrent phenomenon in lung cancer (Figure  
18 1A). However, the lack of similarity between the NCI-MD and TCGA non-tumor samples  
19 may be attributed to the TCGA data being derived from multiple sample populations in  
20 the U.S., differences in sample prep and in sequencing platforms, as illustrated by Meisel  
21 et al. [26].

22 To identify ecological diversity changes associated with lung cancer, we next examined  
23 the richness (Chao1) and diversity (Inverse Simpson) of the microbiome within samples



1 (alpha diversity) of non-disease (immediate autopsy and hospital biopsy) lung tissues,  
2 non-tumor adjacent and tumor tissues from 16S rRNA gene sequencing (NCI-MD study).  
3 Specifically, Chao1 measurement demonstrated a significant increase in both tumor and  
4 non-tumor tissue richness as compared to immediate autopsy control tissue samples  
5 (Figure 1B). Similarly, using the Inverse Simpson index, which measures number  
6 (richness) and abundance (evenness) of species, we observed a significant increase in  
7 alpha diversity in both tumor and non-tumors as compared to hospital biopsy control  
8 tissues (Figure 1B), similar to studies of severe COPD [27] indicating that microbial  
9 diversity of lung cancer tissues are altered from its non-diseased state. However, we did  
10 not see any significant changes in alpha diversity by smoking status (never, former or  
11 current) nor correlation with time since quitting smoking (see Additional file 1: Figure S3),  
12 in cancer-free or lung cancer tissues as has been demonstrated in other lung microbiome  
13 studies [28, 29]. We also asked whether there were differences between microbial  
14 communities using beta diversity (Bray Curtis). Within the NCI-MD study we observed  
15 significant differences in beta diversity between all tissue types (PERMANOVA  $F=2.90$ ,  
16  $P=0.001$ ), tumor and non-tumor (PERMANOVA  $F=2.94$ ,  $P=0.001$ ) and AD v SCC  
17 (PERMANOVA  $F=2.27$ ,  $P=0.005$ ), with tumor vs. non-tumor having the largest among-  
18 group distance denoted by the higher  $F$  value (data not shown). Similarly, we observed  
19 significant difference in beta diversity between tumor and non-tumor (PERMANOVA  
20  $F=3.63$ ,  $P=0.001$ ) and AD v SCC (PERMANOVA  $F=27.19$ ,  $P=0.001$ ) in addition to lung  
21 resection location (upper, lower, left, right) (PERMANOVA  $F=1.36$ ,  $P=0.061$ ) (data not  
22 shown). Together, these data illustrate a trend of increasing diversity and richness  
23 associated with lung cancer.

1 **A distinct group of taxa are enriched with squamous cell carcinoma (SCC) with**  
2 ***Acidovorax* more abundant in smokers.** The two most common types of non-small cell  
3 lung cancer are SCC and AD, arising centrally from the cells lining the bronchi and from  
4 peripheral airways, respectively. Previous studies report that the microbial community  
5 differs between the bronchi and lower lungs in COPD [6]. This phenomenon of anatomic-  
6 specific microbial variation was also apparent in the abundance of genera between  
7 bronchial and SCC tumors from the upper lungs with higher abundance of *Acidovorax* in  
8 comparison to AD tumors (see Additional file 1: Figure S4). Further, the taxonomic  
9 distribution in AD tumors appears more similar to the taxonomic abundance in COPD,  
10 which is generally dominated by *Pseudomonas* [6]. Given this distinction, we controlled  
11 for this potential confounder of lung location in subsequent analyses. This led us to  
12 investigate the specific taxonomic pattern further and ask if there was a specific microbial  
13 consortia that is enriched in SCC or AD tumor tissue. In the NCI-MD study we identified  
14 32 genera that were differentially abundant in SCC (n=47) vs AD (n=67) tumors (Student's  
15 t-test; MW  $P < 0.05$ ), 9 of which were significant after multiple testing correction (FDR)  
16 (*Acidovorax*, *Brevundimonas*, *Comamonas*, *Tepidimonas*, *Rhodoferax*, *Klebsiella*,  
17 *Leptothrix*, *Polaromonas*, *Anaerococcus*) (Figure 2A). We also validated these same  
18 observations in the TCGA data set (AD=485, SCC=489) (Mann-Whitney FDR corrected  
19 p-value < 0.05) (Figure 2B). To control for potential confounders of this association,  
20 including age, gender, race, smoking, anatomical location and stage, we conducted  
21 adjusted logistic regression analysis in the NCI-MD study for each taxa separately and  
22 confirmed 6/9 of these genera were significantly associated with increased odds of being  
23 SCC as compared to AD lung cancer (Figure 2C and see Additional file 1: Table 5).

1 Though we had reduced power, we asked whether the time since quitting smoking would  
2 change this association, and found that *Acidovorax*, *Klebsiella*, *Tepidimonas*,  
3 *Rhodoferax*, and *Anaerococcus* remained significant. When we examined the larger  
4 TCGA data set, we also found significantly increased odds of being SCC as compared  
5 with AD among 4/9 (*Acidovorax*, *Klebsiella*, *Rhodoferax*, *Anaerococcus*) of the same  
6 genera in adjusted models (FDR corrected  $P < 0.05$ ) (Figure 2D and see Additional file 1:  
7 Table 6). This association also remained significant after adjusting for pack years and  
8 time since quitting smoking. Together these data, validated in two separate cohorts,  
9 demonstrate that a specific community of taxa is more abundant in SCC as compared  
10 with AD lung cancer tissue, and are capable of distinguishing between AD and SCC  
11 tumors from individuals with similar exposure to cigarette smoke. However, whether this  
12 is a cause or consequence of the development of SCC cancer remains unknown.

13 Both SCC and AD lung cancers are associated with smoking, however, the association  
14 between smoking and SCC is stronger [30], which lead us to ask whether any of the SCC-  
15 enriched taxa were also associated with smoking. We stratified the tumor samples into  
16 never smokers ( $n=7$ ) or ever-smokers (current ( $n=70$ ) and former smokers ( $n=40$ )) using  
17 linear discriminant analysis (LEfSe) to identify smoking-associated microbial biomarkers  
18 in SCC tumors. We identified 6 genera that were able to distinguish ever (former and  
19 current) vs non-smokers in our NCI-MD study (*Acidovorax*, *Ruminococcus*, *Oscillospira*,  
20 *Duganella*, *Ensifer*, *Rhizobium*) (see Additional file 1: Figure S4C). Specifically,  
21 *Acidovorax* was more abundant in former and current smokers as compared with never  
22 smokers (Kruskal-Wallis  $p$ -value  $< 0.05$ ) (Figure 3A), with a similar trend observed in  
23 TCGA data set ( $n_{\text{never}}=120$ ,  $n_{\text{former}}=551$ ,  $n_{\text{current}}=217$ ) (Kruskal-Wallis  $P=0.27$ ; ANOVA

1  $P=0.02$ ). We did not, however, observe any correlation between *Acidovorax* abundance  
2 and smoking time cessation. Interestingly, the relative abundance of *Acidovorax* and  
3 *Klebsiella* were higher in former and current smokers when we stratified by histological  
4 subtype in both NCI-MD and TCGA data set (Figure 3B, see Additional file 1: Figure S5),  
5 indicating not only are there bacteria which have a higher relative abundance in tumors  
6 from individuals who smoke, but SCC tumors from smokers have even greater relative  
7 abundance of these bacteria. We also demonstrated the presence of this bacterium in  
8 lung tumors using FISH (Figure 3C-D and see Additional file 1: Figure S6), and using  
9 PacBio sequencing, which identified the species as *A. temperans* (see Additional file 1:  
10 Table 4). We did not find any significant associations between pack years or time since  
11 quitting smoking and the abundance of these taxa in either study among SCC tumors in  
12 either study.

13 ***TP53* mutations are associated with enrichment of SSC enriched taxa.** The most  
14 prevalent somatic mutation in SCC lung tumors is in the gene *TP53* [31]. Previous studies  
15 demonstrate that mutations in *TP53*, specifically in colon cancer, lead to disruption of the  
16 epithelial barrier allowing the infiltration of tumor-foraging bacteria and resulting in disease  
17 progression [17]. Given that *TP53* mutations are found in 75-80% of SCC tumors, we  
18 hypothesized that these SCC-associated taxa may be more abundant in tumors with  
19 *TP53* mutations, owing to the loss of the epithelial barrier function in these tumors. To  
20 address this question, we investigated the association between *TP53* mutations in both  
21 NCI-MD (n=107) and TCGA (n=409) data sets using either *TP53* specific sequencing  
22 (MiSeq) or the published *TP53* mutation analysis data from TCGA [31]. We first analyzed  
23 all tumors in the NCI-MD study regardless of histology and identified a group of taxa that

1 were more abundant in tumors with *TP53* mutations (Figure 4A). To have greater power,  
2 we performed the same analysis in the TCGA data set and observed a significant increase  
3 in these same taxa (MW FDR corrected  $P < 0.05$ ) (Figure 4B). When analyzing only SCC  
4 tumors (n=46), this signature became stronger in tumors with *TP53* mutations in both data  
5 sets, specifically among the SCC-associated taxa previously identified (Figure 4C-D). In  
6 the NCI-MD study we found that 5/9 of the genera (*Acidovorax*, *Klebsiella*, *Rhodofera*,  
7 *Comamonas*, and *Polaromonas*) that differentiated SCC from AD were also more abundant  
8 in the tumors harboring *TP53* mutations, though not statistically significant (Figure 4C).  
9 In the TCGA data set, the fold change in all 5 SCC-associated genera were significantly  
10 higher in SCC tumors (n=177) with *TP53* mutations (MW corrected FDR  $< 0.01$ ; Figure  
11 4D). Furthermore, using these same SCC-associated taxa we observed no pattern of  
12 association in AD tumors with *TP53* mutations indicating this signature was specific to  
13 SCC with *TP53* mutations (see Additional file 1: Figure S7A-B). Overall, these data are  
14 consistent with the hypothesis that mutations in *TP53* are associated with the enrichment  
15 of a microbial consortia that are highly represented in SCC tumors.

## 16 **Conclusions:**

17 Gene-environment interactions have been identified as contributors to cancer incidence  
18 [32], however little is known about gene-microbiome interactions in carcinogenesis. We  
19 demonstrate, a gene-microbiome association in human lung cancer, as well as,  
20 histological evidence of a smoking-associated bacterium, *Acidovorax*. Herein, we identify  
21 a microbial consortia that is associated with a histological subtype of lung cancer, SCC,  
22 which is further enriched in tumors with mutations in *TP53*. Given the strong association  
23 between smoking and development of SCC, it follows that a subgroup of this SCC

1 consortium would also be found in smoking-associated SCC. We validate this assumption  
2 finding *Acidovorax spp.* more abundant in SCC tumors harboring *TP53* mutations, and  
3 confirmed the presence of this genus histologically. These results suggest that smoking  
4 may provide an environment conducive to the growth of *Acidovorax spp.* and similar  
5 species, which can flourish in nutrient depleted environments, like that of the lung. More  
6 important these bacteria are capable of using and degrading environmental toxicants, like  
7 those found in tobacco smoke [33]. Alteration of the microenvironment could allow these  
8 species to become tumor-foraging bacteria once the epithelial barrier defense is lost as  
9 a consequence of mutations in *TP53* and malignant transformation. The counterfactual is  
10 also possible. In other words, overgrowth of *Acidovorax spp.*, as the result of smoking  
11 and epithelial barrier damage, may induce mutations by activation of carcinogens, and  
12 propagation of mutated epithelial cells. Whether these species are simply opportunists or  
13 contribute to lung cancer progression, should be the subject of future investigations.  
14 Collectively, these observations indicate that a state of dysbiosis exists in lung cancer.  
15 The hypothesis generated is that epithelial cells in the lung exposed to tobacco smoke  
16 and/or mutations in *TP53* are invaded by species that take advantage of this new  
17 microenvironment. Notably, individuals harboring mutations in *TP53* with stage I SCC  
18 also have poorer prognosis [34], thus it will be important to determine if any of the species  
19 enriched in SCC are functionally related to reduced survival or simply biomarkers of a  
20 diminished mucosal barrier function. Future studies could test the hypothesis using germ-  
21 free mouse models of lung cancer inoculated with SCC-associated spp. prior to or after  
22 lung tumors are present.

1 Our study indicates that smoking is associated with alterations in relative abundance of  
2 species in SCC tumors. The number one risk factor for lung cancer is tobacco exposure  
3 and is a known factor in chronic lung inflammation. Tobacco and cigarette smoke contain  
4 bacterial products (i.e. LPS) that can cause inflammation, impaired barrier function and  
5 potentially alter the microbiome to influence lung carcinogenesis [8, 35, 36]. Additionally,  
6 tobacco leaves harbor both mold and potentially pathogenic bacteria that can be  
7 transferred in a viable form into the respiratory tract on tobacco flakes inhaled in  
8 mainstream smoke [35, 36]. Further, biologically significant quantities of bacteria are  
9 microaspirated daily in healthy individuals [37], and thus is possible for these species to  
10 accumulate in a pathogen-friendly environment. Given that *Acidovorax spp.*, which have  
11 been identified in 2 common brands of cigarettes [38], have the capacity to metabolize  
12 multiple organic pollutants, like those found in cigarette smoke, it is plausible that smoking  
13 creates an environment that allows this bacterium to outcompete other species for  
14 resources and thus survival [39]. Further, these bacteria are capable of metabolizing  
15 polycyclic aromatic hydrocarbons, which are tobacco smoke carcinogens that can cause  
16 DNA adducts, suggesting they may actually contribute to lung carcinogenesis.

17 Oral and nasal microbiome differences have been observed between smokers and non-  
18 smokers [40, 41]. Whether smoking alters the lung *tissue* microbiome; however, is still  
19 not well understood, especially in the context of disease. From a large study of the naso-  
20 and oropharynx, significant differences in microbial communities were identified between  
21 smokers and non-smokers [42]. Additionally, in a study of non-malignant lung tissue  
22 (n=152), they observed a significant increase in alpha diversity with higher number of  
23 pack years of smoking [43]. While they identified *Acidovorax*, *Anaerococcus* and

1 *Comamonas* in smokers, these taxa did not differentiate smokers and non-smokers in a  
2 *healthy* population. However, in a recent study of non-malignant lung tissue, which  
3 compared tissue to isolated extracellular vesicles (EVs) from tissues, the greater diversity  
4 was identified specifically in EVs, with a greater abundance of *Acidovorax* specifically  
5 found in the EVs of smokers, indicating a possible factor in differential findings [44]. These  
6 data indicate that smoking alone may be insufficient to alter the microbial population in a  
7 healthy population. However, smoking has been shown to suppress the immune system  
8 and induce epithelial barrier dysfunction [45]. These factors may allow taxa direct access  
9 to epithelial cells where microbial toxins or reactive oxygen/nitrogen from the  
10 aforementioned species to directly or indirectly encourage malignant transformation of  
11 the lung epithelium via DNA damage and mutations in *TP53* [46-48].

12 Several cancers are caused by bacteria and viruses, including cervical cancer (HPV),  
13 liver cancer (HBV), gastric cancer (*H. pylori* and potentially *B. fragilis*). However, very few  
14 microbes have been identified as carcinogenic. In contrast, microbes such as *H. pylori*  
15 and *E. coli* can promote carcinogenesis through modulation of inflammation, reactive  
16 oxygen species, metabolism and protein degradation. Specifically, several species have  
17 been shown to modulate the tumor-suppressor p53 at both the protein and DNA level  
18 [49]. Mutation in *TP53* is a common hallmark of cancer, and in SCC of the lung is found  
19 to be mutated in 70-80% of tumors [31, 50]. Mutation of *TP53* allows the tumor cells to  
20 evade immune surveillance, cell cycle arrest and death, as well as, disrupt endothelial  
21 cell tight junctions[51]. Colorectal carcinomas associated with high abundance of fecal *F.*  
22 *nucleatum* were found to have the highest number of somatic mutations, suggesting that  
23 these mutations create a pathogen-friendly environment [11, 15]. Furthermore, the loss



1 of p53 in enterocytes impairs the epithelial barrier and allows infiltration of bacteria  
2 resulting in NF- $\kappa$ B signaling, which was required for tumor progression [17]. This evidence  
3 suggests that SCC tumors with *TP53* mutations could have poor epithelial barrier  
4 function, thus allowing tumor foraging bacteria, like those identified in our study, to  
5 become more abundant in tumors with *TP53* mutations. The counterfactual is also  
6 possible. Similar to the *B. fragilis* toxin ETBF, which is genotoxic and initiates colon  
7 carcinogenesis in animal models [52], one or more of the tumor-associated species may  
8 induce *TP53* mutations. Whether any of these bacteria are promoting SCC tumorigenesis  
9 or inducing mutations in *TP53* is currently under investigation.

10 With the majority of lung cancer being diagnosed at late stage, the recent advancement  
11 in the treatment of late stage (III/IV) lung cancer with immune checkpoint inhibitors  
12 targeting PD-1, nivolumab, has resulted in a 40% reduced risk of death as compared to  
13 standard chemotherapy [53]. The response rate, however, is still not complete for these  
14 patients. Important insights into understanding the differential response rates of this new  
15 immunotherapy has suggested the composition of the lung microbiome prior to therapy  
16 as a key player in therapeutic effectiveness [54]. Given our results demonstrating  
17 alterations in the microbial composition in lung cancer that are histology and mutation  
18 specific, future studies should address whether the lung or nasal microbiome composition  
19 improves the stratification of patients who would be most responsive to immunotherapy.

20 This suggestion is supported by recent animal studies demonstrating the contribution of  
21 the gut microbiome to the effectiveness of immunotherapy [55].

22 The strength of our findings include the large number of individuals sampled in this study,  
23 use of two separate sample populations, two sets of control populations, two separate

1 sequencing methodologies (MiSeq and PacBio) and microscopic validation (FISH) of the  
2 species in lung tumor tissue. We have also been diligent in assessing the possibility of  
3 contaminating taxa being an artifact of sample collection or sample processing by  
4 sequencing across 2 different platforms, and microscopy, although we cannot rule that  
5 possibility out entirely. While we were able to control for antibiotic exposure in the NCI-  
6 MD study, we acknowledge a limitation of the validation study is the inability to control for  
7 antibiotic exposure in the TCGA dataset, as well as, significant differences in clinical  
8 features between the cancer cases and controls, which could be confounders. However,  
9 in a recent study of the microbiome of endoscopic gastric biopsies, confirmation of  
10 multiple shared bacteria in clinical samples, specifically *H. pylori*, was demonstrated using  
11 the TCGA RNA-seq data with methods similar to those presented in our study [56].

12 With these results, we foresee a new avenue for mechanistic studies to address the role  
13 of microbe-host relationship in lung cancer inflammation, response to therapy, and  
14 microbial engineering for drug delivery.

## 15 **Methods:**

16 **Sample Populations and data sets:** Samples used for DNA extraction, PCR and  
17 sequencing were obtained from the ongoing NCI-MD study (7 hospitals participating in  
18 the greater Baltimore, MD area recruited from 1999 to 2012), as described  
19 previously [57], from which 398 lung cancer cases were obtained, and included both  
20 tumor and non-tumor adjacent, with 121 matched pairs. The final sample set used for  
21 analysis after sequencing, which contained 106 matched pairs after quality control, is  
22 found in See Additional file 1: Table 1. Lung tumors and paired non-tumor adjacent  
23 samples from the NCI-MD study were obtained at the time of surgery, from which

1 a section of tumor and non-involved adjacent lung tissue were flash frozen and  
2 stored at -80 degrees. At the time of study entry, a detailed patient interview was  
3 conducted to obtain basic clinical information in addition to previous cancers, neo-  
4 adjuvant therapies, current medications, family history of cancer, smoking history,  
5 education level and financial status. Staging was assigned using the Cancer Staging  
6 Manual of the American Joint Committee on Cancer (AJCC) 7th edition. Pre-operative  
7 antibiotics were administered for those cases recruited after 2008 and any antibiotic oral  
8 medication use was used as a co-variate for all statistical analysis in model testing,  
9 however these data were not available for immediate autopsy (ImA) non-cancer  
10 samples. Controls representing non-cancerous tissue were obtained from the Lung  
11 Cancer Biorepository Research Network (n=16; hospital controls). These samples were  
12 obtained as frozen lung specimens from individuals who had a previous positive nodule  
13 identified by PET scan, and subsequently underwent tissue biopsy, which was ruled  
14 benign. Clinical information included those listed above as well as smoking history,  
15 antibiotic usage (Y/N), and disease diagnosis. Two cases had emphysema at the time of  
16 biopsy and were not used in the analyses. Immediate autopsy (ImA) samples obtained  
17 from the University of Maryland (UMD) hospital, which is part of the NCI-MD study  
18 population (n=41; population controls) (See Additional file 1: Table 1). Lung tissue from  
19 ImA was received frozen from the UMD biorepository and served as the population  
20 controls for non-cancer lung tissue. Briefly, samples from ImA were obtained within  
21 minutes (<30 min.) after death and put on ice for dissection or frozen to -80 degrees. All  
22 ImA subjects underwent extensive autopsy and were determined to be cancer free.  
23 Demographic information included age, gender, race and cause of death only. Non-

1 smokers in the NCI-MD study were categorized as having smoked <100 cigarettes or  
2 fewer than 5 packs over a lifetime, whereas smokers were categorized as current  
3 smokers or former smokers, which had quit for > 6 months. Sequences derived from  
4 RNA-seq of lung tumor (n=1006) or non-tumor adjacent tissue (n=106) were obtained  
5 from The Cancer Genome Atlas (N=1112) for validation of the NCI-MD study 16S rRNA  
6 gene sequencing analysis and results. Due to the fact that all RNA-seq data in TCGA  
7 were obtained using poly-A capture, any microbial data from this analysis will necessarily  
8 be biased. For this reason, we only used these data as validation of results first identified  
9 in our 16S rRNA gene sequencing analysis. Public data, including all clinical patient  
10 information (See Additional file 1: Table 1), was downloaded from the Data Matrix on the  
11 TCGA website, [https://tcga-  
12 data.nci.nih.gov/tcga/dataAccessMatrix.htm](https://tcga-data.nci.nih.gov/tcga/dataAccessMatrix.htm). The raw data  
13 in the form of BAM and FastQ files were downloaded from a secure server at CGHUB, and  
14 access was applied for and approved for raw data downloads by University of California  
15 Santa Cruz, <https://cghub.ucsc.edu/>. The files were downloaded and stored in archived  
16 format and subsequently un-archived for analysis. The results shown here are in whole  
17 or part based upon data generated by the TCGA Research Network:  
18 <http://cancergenome.nih.gov/>

18 **DNA extraction and 16S rRNA gene sequencing:** DNA from lung cancer and control  
19 lung tissues was isolated according to a tissue-modified version of the standard Human  
20 Microbiome Project's DNA isolation procedure. Genomic DNA from frozen lung tissue  
21 was extracted after tissue homogenization in Yeast Cell Lysis Buffer (EpiCentre)  
22 containing lysozyme (EpiCentre) by bead beating (TissueLyser II) with proteinase k  
23 (Invitrogen). DNA was purified with the Life Technologies PureLink kit according the

1 manufacturer's protocol (Invitrogen). A sterile water control (MoBio) was also processed  
2 along with all frozen tissue and used as background contamination control for DNA  
3 isolation, PCR and sequencing. Background contamination controls for tissue collection,  
4 pathology and sequencing were also collected through routine swabs after surgery and  
5 sequenced in conjunction with tissue samples. Specifically, the NCI-MD study tissues  
6 were isolated in a laminar flow hood to minimize contamination for downstream  
7 applications, using sterile forceps and gloves. Controls for contamination points during  
8 surgical tissue collection and pathological assessment included swabs from inside of the  
9 surgical tissue collection vessel before/after, pathology cutting board before/after,  
10 pathology knife blade before/after, gloves before/after, pathology ink bottle rim and  
11 collection tube for freezing before/after (See Additional file 1: Dataset 1). Briefly, swabs  
12 were dipped in Yeast cell Lysis buffer and area/object swabbed, then the swab was  
13 broken off into tube and frozen at -80. A negative control was also collected using 50  $\mu$ L  
14 of MoBio PCR water as a mock sample (PCR\_NC) and processed through DNA  
15 extraction with tissues to assess contamination from reagents, which was analyzed on  
16 three separate runs of MiSeq. The positive control was the High Even Mock Community  
17 (Broad Institute), which was also sequenced on three separate runs of MiSeq. The  
18 negative and positive control samples were spiked into four MiSeq runs at a similar  
19 concentration to that of the NCI-MD samples. To control for false grouping or batch  
20 affects, we randomized the tissue sample types (non-tumor (NT), tumor (T), immediate  
21 autopsy (ImA)) (with the exception of HB controls) across 5 separate sequencing runs of  
22 MiSeq (See Additional file 1: Dataset 2). The fifth plate consisted of duplicate samples  
23 and samples that had failed sequencing on previous runs of MiSeq.

1 Sequencing for the 16S rRNA gene was performed with 40 ng of sample DNA from 398  
2 cases and 57 controls using primers for variable region V3-V5 with 16S rRNA gene  
3 sequence-specific portions based on Kozich et al. [58] with adapters for subsequent  
4 addition of standard Illumina dual indexes. PCR was performed using a Phusion DNA  
5 Polymerase High Fidelity kit (ThermoFisher). The cycling conditions were as follows: 98  
6 °C for 2 min, then 36 cycles of 98 °C for 15 s, 60 °C for 1 min 40 s, and 74 °C for 1 min.  
7 PCR products were purified using the Agencourt AMPure XP kit according to the  
8 manufacturer's instructions (Beckman Coulter). Second round PCR with Illumina dual-  
9 index oligos was performed using a Phusion DNA Polymerase High Fidelity kit  
10 (ThermoFisher) as following: 98 °C for 2 min, then 6 cycles of 98 °C for 15 s, 72 °C for 20  
11 s, and 72 °C for 1 min. Samples were pooled, purified using Agencourt AMPure XP.  
12 Sequencing was conducted on Illumina MiSeq instrument using v3 600 cycles kit (see  
13 Additional file 1: Methods).

14 **Full-length 16S rDNA PCR reactions (PacBio):** Full-length 16S amplifications were  
15 performed using: 1µl of total DNA as template; 0.25 µM of the universal 16S primers F27  
16 and R1492 with four different sets of asymmetric barcodes at (see Additional file 1: Table  
17 7). and GoTaq Hot Start Master Mix (Promega) in a 50µl final volume. Cycling conditions  
18 were: 94 °C, 3 min; 35 cycles of 94 °C 30 sec, 54 °C 30 sec, 72 °C 2 min; following by a  
19 5 min final elongation at 72 °C. PCR products were cleaned with AxyPrep™ MagPCR  
20 (Corning Life Sciences) according to the manufacturer's protocol and eluted in 40µl of  
21 water. Cleaned PCR products were quantified using the Bio-Rad QX200 droplet digital  
22 PCR (Bio-Rad) and QX200 EvaGreen® Supermix with primers F357 and R534 (see  
23 Additional file 1: Table 8) targeting the V3 variable region of 16S rDNA. Based on the

1 results, amplicon libraries were normalized to the same concentration prior to pooling.  
2 Pooling was always performed using amplicon libraries with distinct barcodes.  
3 Multiplexing was performed with 2-4 libraries per pool.  
4 **Pacific Biosciences circular consensus sequencing:** Sequencing library construction  
5 was accomplished using the Pacific Biosciences (PacBio) SMRTbell™ Template Prep Kit  
6 V1 on the normalized pooled PCR products. Sequencing was performed using the PacBio  
7 RS II platform using protocol “Procedure & Checklist - 2 kb Template Preparation and  
8 Sequencing” (part number 001-143-835- 06). DNA Polymerase Binding Kit P6 V2 was  
9 used for sequencing primer annealing and polymerase binding. SMRTbell libraries were  
10 loaded onto SMRTcells V3 at a final concentration of 0.0125 nM using the MagBead kit,  
11 as determined using the PacBio Binding Calculator software. Internal Control Complex  
12 P6 was used for all reactions to monitor sequencing performance. DNA Sequencing  
13 Reagent V4 was used for sequencing on the PacBio RS II instrument, which included  
14 MagBead loading and stage start. Movie time was 3 hrs for all SMRTcells. PacBio  
15 sequencing runs were set up using RS Remote PacBio software and monitored using  
16 RS Dashboard software. Sequencing performance and basic statistics were collected  
17 using SMRT® Analysis Server v2.3.0. De-multiplexing and conversion to FastQ was  
18 accomplished using the Reads of Insert (ROI) protocol in the SMRT portal v2.3 software.  
19 Only reads with a minimum of 5 circular passes and a predicted accuracy of 90 (PacBio  
20 score) or better were used for further analysis. Each read was labelled in the header with  
21 the number of CCS (circular consensus sequence) passes and the sample designation  
22 using a custom ruby script, followed by concatenation of all reads into a single file for  
23 subsequent filtering and clustering.

1 **Filtering and OTU clustering of 16S rRNA gene sequence data:** Initial screening for  
2 length and quality using QIIME (qiime.org) [59]. Reads containing more than five  
3 consecutive low quality base calls (Phred < Q20), were truncated at the beginning of the  
4 low quality region. Due to the low quality of the majority of R2 reads (Phred < Q20 and  
5 <150bp length), we used the R1 reads only for this analysis. Passing sequences were  
6 required to have high quality base calls ( $\geq$  Phred Q20) along a minimum of 75% of the  
7 read length to be included. After primer removal, final sequences containing ambiguous  
8 bases (Ns) or lengths less than 150bp were removed. High quality sequences were then  
9 screened for spurious PhiX contaminant using BLASTN with a word size of 16. Reads  
10 were then assessed for chimeras using USEARCH61 (de novo mode, 97% identity  
11 threshold for clustering). Non- chimeric sequences were screened for contaminant  
12 chloroplast and mitochondria using the RDP naïve Bayesian classifier, as well as non-  
13 specific human genome contaminant using Bowtie2 against the UCSC hg19 reference  
14 sequence. Finally, sequences were evaluated for residual contaminants using BLASTN  
15 searches of the GreenGenes database (v13.5). Filtered reads included those not  
16 matching any reference with at least 70% identity along 60% of their length. Exploratory  
17 assessment using BLASTN searches against the NCBI NT database indicated the  
18 majority unknown contaminant reads were amplified human genome sequence. High-  
19 quality passing sequences were subsequently clustered into operational taxonomic units  
20 using the open-reference operational taxonomic unit (OTU) picking methodology  
21 implemented within QIIME using default parameters and the GreenGenes database (99%  
22 OTUs) supplemented by reference sequences from the SILVA database (v111). Prior to  
23 downstream diversity analyses, the OTU table was rarefied to 5,500 sequences per



1 sample. Prior to diversity analysis, contaminants were removed and again OTUs table  
2 rarified to 5,500 sequences per sample. Alpha diversity estimators and beta-diversity  
3 metrics were computed in QIIME with differential abundance analyses performed in R. In  
4 order to determine significant differences in beta diversity, we used the adonis function in  
5 the R package vegan to conduct PERMANOVA with Bray Curtis distance and 999  
6 permutations. All sequences from MiSeq and PacBio data sets have been deposited at  
7 the following location: <http://www.ncbi.nlm.nih.gov/bioproject/320383>. See Additional file  
8 1: Methods for details regarding PacBio sequence processing.

9 **TCGA RNA-seq data processing and alignment:** In order to analyze all RNA-seq  
10 unmapped reads from TCGA lung cancer samples, we developed a custom metagenomic  
11 analysis pipeline using (i) MetaPhlan2, (ii) Kraken, and (iii) Pathoscope [22]. First, all  
12 reads were filtered for quality using Trimmomatic (v0.32, minimum average quality >  
13 20 over a 5bp sliding window, minimum final length <sup>3</sup> 28bp) and searched for potential  
14 PhiX-174 contaminant using Bowtie2. Reads passing this filter were then mapped to  
15 the comprehensive NCBI Homo sapiens Annotation (Release 106) using Bowtie2  
16 to remove any human-associated reads. The resulting non-human read set was  
17 then taxonomically assigned using (i) MetaPhlan2, (ii) Kraken, and (iii) Pathoscope in  
18 parallel to evaluate consistency in the resulting profiles. Assignments from each  
19 method were aggregated at higher taxonomic levels (genus and species) for  
20 downstream statistical comparisons. The results from Pathoscope and its validation  
21 in other studies lead us to use these data for the remainder of the downstream analysis.

1 Alpha diversity estimators and beta-diversity (Bray Curtis) metrics were computed in  
2 QIIME using genus and species level assignments with differential abundance analyses  
3 performed in R and Stata (v13).

4 **Statistical Analysis and Classification of Taxa Associated with Lung Cancer:** Alpha  
5 and beta-diversity metrics were computed in QIIME with differential abundance analyses  
6 performed in R and Stata (v13). Mann-Whitney tests corrected for multiple testing  
7 (Benjamini–Hochberg (FDR)) were used to conduct initial comparisons between tissue  
8 type and histological subtype (AD or SCC) followed by multivariable logistic regression  
9 controlling for multiple confounders. A logistic regression model was constructed to  
10 estimate the odds of AD vs SCC for each taxa stratified by mutation status with and  
11 interaction term between the taxa and mutation added to the model. See See Additional  
12 file 1: Methods for details.

13 **TP53 gene sequencing and mutation analysis:** Genomic DNA extracted from lung  
14 cancer tissues (n=107) was submitted for *TP53*-targeted sequencing using the MiSeq  
15 Illumina platform. For mutation analysis, 46 samples were SCC. The assay was targeted  
16 at the exons and proximal splice sites. Forward and reverse primers were tailed with  
17 Illumina Adapter tags for downstream next generation sequencing using the BioMark HD  
18 System (Fluidigm) and Access Array IFC chips and kits (Fluidigm). PCR products were  
19 indexed using an 8-mer oligo barcode. See Additional file 1: Table 3 lists sequences for  
20 primers used in the sequencing assay. Sequence results were processed and aligned to  
21 human genome and underwent QC requiring coverage > 100 reads with the variant (most  
22 SNVs had a read depth in the thousands) and minimum allele frequency > 10%. The 100-  
23 level cutoff for coverage allows to detect variations if the tumor fraction >~ 20% with 95%

1 confidence, under the assumption of a diploid genome. The 10% allele frequency cutoff  
2 is derived from that same consideration. The variants called included all common  
3 polymorphisms. Because only tumor was sequenced, in order to score somatic mutations,  
4 those deemed to be germline were filtered out. These included SNVs present in dbSNP  
5 with high reported allele frequency (common polymorphisms). Also, SNVs in untranslated  
6 regions and introns were not considered, as their somatic status and functional  
7 implications are unclear. The presence of putative somatic exonic and splicing variants  
8 was corroborated in TCGA and COSMIC datasets. See Additional file 1: Table 2 for  
9 details.

10 **Fluorescent *in situ* hybridization analysis of *Acidovorax*:** In order to confirm the  
11 presence *Acidovorax* in lung tumor tissue, fluorescently labeled probes were created for  
12 each bacterium. Genus or species-specific bacteria probes were hybridized using tumor  
13 tissues in addition to gram stain on each. Tumor tissues from cancer cases were fixed in  
14 OCT and sectioned frozen (10  $\mu$ m). Prior to fixation in 4% paraformaldehyde sections  
15 were thawed at RT. Sections were washed in PBS and the probe (2  $\mu$ L) was added to 90  
16  $\mu$ L FISH buffer (0.9 M NaCl, 0.02 M Tris pH 7.5, 0.01% SDS, 20% formamide). This  
17 solution was added to the section (20-100  $\mu$ L) and placed in the hybridization chamber  
18 (46°C) for 3- 18 hrs depending on probe used. Section were washed with twice (wash 1  
19 - 0.9 M NaCl, 0.02 M Tris pH 7.5, 0.01% SDS, 20% formamide; wash 2 - 0.9 M NaCl,  
20 0.02 M Tris pH 7.5, 0.01% SDS) and incubated at 48°C for 15 min. Slides were then dried  
21 for 10 min. Prior to visualization, DAPI and Vectashield was added slides. The probe used  
22 for FISH was: *Acidovorax* (CTT TCG CTC CGT TAT CCC, 5' modification: Alexa Fluor  
23 532). Representative fields were imaged using Zeiss 710 and a 100X objective for the

1 probe. In addition to 2D images, Z stacks were also obtained for each bacterial probe and  
2 used to reconstruct 3D images and movies using Imaris software. Quantification of  
3 *Acidovorax* probe reactivity was conducted using 10 2D fields of two patients. At least  
4 300 cells were counted per patient. Percentage (%) of cells with perinuclear probe  
5 reactivity was quantified using ImagePro Plus 6.0 software.

## 6 **Declarations:**

7 **Ethics approval and consent to participate:** This study was approved by the  
8 Institutional Review Board at the NIH and all individuals participating in the NCI-MD case-  
9 control study signed informed consents for the collection of biospecimens, personal and  
10 medical information.

11 **Consent for publication:** Not applicable.

12 **Availability of data and material:** All de-identified data from this study will be made  
13 available upon reasonable request. Specifically, all sequencing data has been deposited  
14 under the bioproject number 320838 and is publically available at the following location:  
15 <http://www.ncbi.nlm.nih.gov/bioproject/320383>.

16 **Competing interests:** James White is a significant shareholder in the company  
17 Resphera Insight Inc. All other authors declare no conflicts of interest.

18 **Funding:** This work was supported by intramural funding from the National Cancer  
19 Institute, National Institutes of Health, Bethesda, MD. Work by L. G. and A. Vargas. were  
20 also supported by the Cancer Prevention Research Program fellowship at the National  
21 Cancer Institute, National Institutes of Health, Bethesda, MD.

22 **Authors' contributions:** KLG, JAS and CCH conceived of the study, experiments,  
23 analyzed data, interpreted results and participated in writing and review; CD, SC, JO,

1 AIR, VVB, MAP, SB, PSM, JEK, SVB, ASB, JPE, JCM, GDE, JAS and JRW sequenced  
2 samples and/or processed sequencing data and mutation analysis, and JRW, AJV and  
3 ECP conducted statistical analysis of data; AV, JAB, NM, TC, ANH, TMS, and MRW  
4 conducted FISH experiments and interpreted results; EDB and MAK provided assistance  
5 with procuring and processing biospecimens and clinical databases; BMR, AHD, and GT  
6 provided technical and data interpretation assistance and manuscript review. All authors  
7 read and approved the final manuscript.

8 **Acknowledgements:** We thank the University of Maryland Cancer Studies Team  
9 directed by Dean Mann, for their support, including Steven Schech for the collection of  
10 background swabs and specimens.

11

## 12 **References:**

- 13 1. AMC: **Cancer Facts and Figures**. American Cancer Society; 2014.
- 14 2. Sugimura H, Yang P: **Long-term survivorship in lung cancer: a review**. *Chest*  
15 2006, **129**:1088-1097.
- 16 3. Boursi B, Mamtani R, Haynes K, Yang YX: **Recurrent antibiotic exposure may**  
17 **promote cancer formation--Another step in understanding the role of the**  
18 **human microbiota?** *Eur J Cancer* 2015, **51**:2655-2664.
- 19 4. Dickson RP, Erb-Downward JR, Martinez FJ, Huffnagle GB: **The Microbiome**  
20 **and the Respiratory Tract**. *Annu Rev Physiol* 2016, **78**:481-504.
- 21 5. Dickson RP, Erb-Downward JR, Huffnagle GB: **The role of the bacterial**  
22 **microbiome in lung disease**. *Expert Rev Respir Med* 2013, **7**:245-257.
- 23 6. Erb-Downward JR, Thompson DL, Han MK, Freeman CM, McCloskey L, Schmidt  
24 LA, Young VB, Toews GB, Curtis JL, Sundaram B, et al: **Analysis of the lung**  
25 **microbiome in the "healthy" smoker and in COPD**. *PLoS One* 2011,  
26 **6**:e16384.
- 27 7. Twomey KB, Alston M, An SQ, O'Connell OJ, McCarthy Y, Swarbreck D, Febrer  
28 M, Dow JM, Plant BJ, Ryan RP: **Microbiota and metabolite profiling reveal**  
29 **specific alterations in bacterial community structure and environment in**  
30 **the cystic fibrosis airway during exacerbation**. *PLoS One* 2013, **8**:e82432.
- 31 8. Heijink IH, Brandenburg SM, Postma DS, van Oosterhout AJM: **Cigarette**  
32 **smoke impairs airway epithelial barrier function and cell-cell contact**  
33 **recovery**. *European Respiratory Journal* 2012, **39**:419-428.

- 1 9. Venkataraman A, Rosenbaum MA, Werner JJ, Winans SC, Angenent LT:  
2 **Metabolite transfer with the fermentation product 2,3-butanediol enhances**  
3 **virulence by *Pseudomonas aeruginosa*. *ISME J* 2014, **8**:1210-1220.**
- 4 10. Shiels MS, Albanes D, Virtamo J, Engels EA: **Increased risk of lung cancer in**  
5 **men with tuberculosis in the alpha-tocopherol, beta-carotene cancer**  
6 **prevention study. *Cancer Epidemiol Biomarkers Prev* 2011, **20**:672-678.**
- 7 11. Kostic AD, Chun E, Robertson L, Glickman JN, Gallini CA, Michaud M, Clancy  
8 TE, Chung DC, Lochhead P, Hold GL, et al: ***Fusobacterium nucleatum***  
9 **potentiates intestinal tumorigenesis and modulates the tumor-immune**  
10 **microenvironment. *Cell Host Microbe* 2013, **14**:207-215.**
- 11 12. McCoy AN, Araujo-Perez F, Azcarate-Peril A, Yeh JJ, Sandler RS, Keku TO:  
12 ***Fusobacterium* is associated with colorectal adenomas. *PLoS One* 2013,**  
13 ****8**:e53653.**
- 14 13. Rubinstein MR, Wang X, Liu W, Hao Y, Cai G, Han YW: ***Fusobacterium***  
15 ***nucleatum* promotes colorectal carcinogenesis by modulating E-**  
16 **cadherin/beta-catenin signaling via its FadA adhesin. *Cell Host Microbe***  
17 **2013, **14**:195-206.**
- 18 14. Strauss J, Kaplan GG, Beck PL, Rioux K, Panaccione R, Devinney R, Lynch T,  
19 Allen-Vercoe E: **Invasive potential of gut mucosa-derived *Fusobacterium***  
20 ***nucleatum* positively correlates with IBD status of the host. *Inflamm Bowel***  
21 ***Dis* 2011, **17**:1971-1978.**
- 22 15. Tahara T, Yamamoto E, Suzuki H, Maruyama R, Chung W, Garriga J, Jelinek J,  
23 Yamano HO, Sugai T, An B, et al: ***Fusobacterium* in colonic flora and**  
24 **molecular features of colorectal carcinoma. *Cancer Res* 2014, **74**:1311-1318.**
- 25 16. Sears CL, Geis AL, Housseau F: ***Bacteroides fragilis* subverts mucosal**  
26 **biology: from symbiont to colon carcinogenesis. *J Clin Invest* 2014,**  
27 ****124**:4166-4172.**
- 28 17. Schwitalla S, Ziegler PK, Horst D, Becker V, Kerle I, Begus-Nahrman Y, Lechel  
29 A, Rudolph KL, Langer R, Slotta-Huspenina J, et al: **Loss of p53 in enterocytes**  
30 **generates an inflammatory microenvironment enabling invasion and lymph**  
31 **node metastasis of carcinogen-induced colorectal tumors. *Cancer Cell***  
32 **2013, **23**:93-106.**
- 33 18. Robles AI, Harris CC: **Clinical outcomes and correlates of TP53 mutations**  
34 **and cancer. *Cold Spring Harb Perspect Biol* 2010, **2**:a001016.**
- 35 19. Oren M, Rotter V: **Mutant p53 gain-of-function in cancer. *Cold Spring Harb***  
36 ***Perspect Biol* 2010, **2**:a001107.**
- 37 20. Trump BF, Valigorsky JM, Dees JH, Mergner WJ, Kim KM, Jones RT,  
38 Pendergrass RE, Garbus J, Cowley RA: **Cellular change in human disease. A**  
39 **new method of pathological analysis. *Hum Pathol* 1973, **4**:89-109.**
- 40 21. Meadow JF, Altrichter AE, Green JL: **Mobile phones carry the personal**  
41 **microbiome of their owners. *PeerJ* 2014, **2**:e447.**
- 42 22. Byrd AL, Perez-Rogers JF, Manimaran S, Castro-Nallar E, Toma I, McCaffrey T,  
43 Siegel M, Benson G, Crandall KA, Johnson WE: **Clinical PathoScope: rapid**  
44 **alignment and filtration for accurate pathogen identification in clinical**

- 1 **samples using unassembled sequencing data.** *BMC Bioinformatics* 2014,  
2 **15:262.**
- 3 23. Huang YJ, Nelson CE, Brodie EL, Desantis TZ, Baek MS, Liu J, Woyke T,  
4 Allgaier M, Bristow J, Wiener-Kronish JP, et al: **Airway microbiota and**  
5 **bronchial hyperresponsiveness in patients with suboptimally controlled**  
6 **asthma.** *J Allergy Clin Immunol* 2011, **127:372-381** e371-373.
- 7 24. Zhao J, Schloss PD, Kalikin LM, Carmody LA, Foster BK, Petrosino JF, Cavalcoli  
8 JD, VanDevanter DR, Murray S, Li JZ, et al: **Decade-long bacterial community**  
9 **dynamics in cystic fibrosis airways.** *Proc Natl Acad Sci U S A* 2012,  
10 **109:5809-5814.**
- 11 25. Hilty M, Burke C, Pedro H, Cardenas P, Bush A, Bossley C, Davies J, Ervine A,  
12 Poulter L, Pachter L, et al: **Disordered microbial communities in asthmatic**  
13 **airways.** *PLoS One* 2010, **5:e8578.**
- 14 26. Meisel JS, Hannigan GD, Tyldsley AS, SanMiguel AJ, Hodkinson BP, Zheng Q,  
15 Grice EA: **Skin Microbiome Surveys Are Strongly Influenced by**  
16 **Experimental Design.** *J Invest Dermatol* 2016, **136:947-956.**
- 17 27. Pragman AA, Kim HB, Reilly CS, Wendt C, Isaacson RE: **The lung microbiome**  
18 **in moderate and severe chronic obstructive pulmonary disease.** *PLoS One*  
19 2012, **7:e47305.**
- 20 28. Segal LN, Alekseyenko AV, Clemente JC, Kulkarni R, Wu B, Gao Z, Chen H,  
21 Berger KI, Goldring RM, Rom WN, et al: **Enrichment of lung microbiome with**  
22 **supraglottic taxa is associated with increased pulmonary inflammation.**  
23 *Microbiome* 2013, **1:19.**
- 24 29. Morris A, Beck JM, Schloss PD, Campbell TB, Crothers K, Curtis JL, Flores SC,  
25 Fontenot AP, Ghedin E, Huang L, et al: **Comparison of the Respiratory**  
26 **Microbiome in Healthy Nonsmokers and Smokers.** *American Journal of*  
27 *Respiratory and Critical Care Medicine* 2013, **187:1067-1075.**
- 28 30. Pesch B, Kendzia B, Gustavsson P, Jöckel K-H, Johnen G, Pohlabeln H, Olsson  
29 A, Ahrens W, Gross IM, Bröske I, et al: **Cigarette smoking and lung cancer—**  
30 **relative risk estimates for the major histological types from a pooled**  
31 **analysis of case–control studies.** *International Journal of Cancer* 2012,  
32 **131:1210-1219.**
- 33 31. **Comprehensive genomic characterization of squamous cell lung cancers.**  
34 *Nature* 2012, **489:519-525.**
- 35 32. Hutter CM, Mechanic LE, Chatterjee N, Kraft P, Gillanders EM, Tank NCIG-ET:  
36 **Gene-environment interactions in cancer epidemiology: a National Cancer**  
37 **Institute Think Tank report.** *Genet Epidemiol* 2013, **37:643-657.**
- 38 33. Darmawan R NH, Ohta H, Niidome T, Takikawa K, and Morimura S: **Isolation**  
39 **and Evaluation of PAH Degrading Bacteria.** *Bioremediation & Biodegradation*  
40 2015, **6:7.**
- 41 34. Ahrendt SA, Hu Y, Buta M, McDermott MP, Benoit N, Yang SC, Wu L, Sidransky  
42 D: **p53 Mutations and Survival in Stage I Non-Small-Cell Lung Cancer:**  
43 **Results of a Prospective Study.** *Journal of the National Cancer Institute* 2003,  
44 **95:961-970.**

- 1 35. Sapkota AR, Berger S, Vogel TM: **Human pathogens abundant in the**  
2 **bacterial metagenome of cigarettes.** *Environ Health Perspect* 2010, **118**:351-  
3 356.
- 4 36. Pauly JL, Paszkiewicz G: **Cigarette smoke, bacteria, mold, microbial toxins,**  
5 **and chronic lung inflammation.** *J Oncol* 2011, **2011**:819129.
- 6 37. Gleeson K, Egli DF, Maxwell SL: **Quantitative aspiration during sleep in**  
7 **normal subjects.** *Chest* 1997, **111**:1266-1272.
- 8 38. Chopyk J, Chattopadhyay S, Kulkarni P, Claye E, Babik KR, Reid MC, Smyth  
9 EM, Hittle LE, Paulson JN, Cruz-Cano R, et al: **Mentholation affects the**  
10 **cigarette microbiota by selecting for bacteria resistant to harsh**  
11 **environmental conditions and selecting against potential bacterial**  
12 **pathogens.** *Microbiome* 2017, **5**:22.
- 13 39. Ertel A, Eng R, Smith SM: **The differential effect of cigarette smoke on the**  
14 **growth of bacteria found in humans.** *Chest* 1991, **100**:628-630.
- 15 40. Morris A, Beck JM, Schloss PD, Campbell TB, Crothers K, Curtis JL, Flores SC,  
16 Fontenot AP, Ghedin E, Huang L, et al: **Comparison of the respiratory**  
17 **microbiome in healthy nonsmokers and smokers.** *Am J Respir Crit Care Med*  
18 2013, **187**:1067-1075.
- 19 41. Wu J, Peters BA, Dominianni C, Zhang Y, Pei Z, Yang L, Ma Y, Purdue MP,  
20 Jacobs EJ, Gapstur SM, et al: **Cigarette smoking and the oral microbiome in**  
21 **a large study of American adults.** *ISME J* 2016, **10**:2435-2446.
- 22 42. Charlson ES, Chen J, Custers-Allen R, Bittinger K, Li H, Sinha R, Hwang J,  
23 Bushman FD, Collman RG: **Disordered microbial communities in the upper**  
24 **respiratory tract of cigarette smokers.** *PLoS One* 2010, **5**:e15216.
- 25 43. Yu G, Gail MH, Consonni D, Carugno M, Humphrys M, Pesatori AC, Caporaso  
26 NE, Goedert JJ, Ravel J, Landi MT: **Characterizing human lung tissue**  
27 **microbiota and its relationship to epidemiological and clinical features.**  
28 *Genome Biol* 2016, **17**:163.
- 29 44. Kim HJ, Kim YS, Kim KH, Choi JP, Kim YK, Yun S, Sharma L, Dela Cruz CS,  
30 Lee JS, Oh YM, et al: **The microbiome of the lung and its extracellular**  
31 **vesicles in nonsmokers, healthy smokers and COPD patients.** *Exp Mol Med*  
32 2017, **49**:e316.
- 33 45. Adar SD, Huffnagle GB, Curtis JL: **The respiratory microbiome: an**  
34 **underappreciated player in the human response to inhaled pollutants?** *Ann*  
35 *Epidemiol* 2016, **26**:355-359.
- 36 46. Nougayrede JP, Homburg S, Taieb F, Boury M, Brzuszkiewicz E, Gottschalk G,  
37 Buchrieser C, Hacker J, Dobrindt U, Oswald E: **Escherichia coli induces DNA**  
38 **double-strand breaks in eukaryotic cells.** *Science* 2006, **313**:848-851.
- 39 47. Putze J, Hennequin C, Nougayrede JP, Zhang W, Homburg S, Karch H, Bringer  
40 MA, Fayolle C, Carniel E, Rabsch W, et al: **Genetic structure and distribution**  
41 **of the colibactin genomic island among members of the family**  
42 **Enterobacteriaceae.** *Infect Immun* 2009, **77**:4696-4703.
- 43 48. Guerra L, Guidi R, Frisan T: **Do bacterial genotoxins contribute to chronic**  
44 **inflammation, genomic instability and tumor progression?** *FEBS J* 2011,  
45 **278**:4577-4588.



- 1 49. Siegl C, Rudel T: **Modulation of p53 during bacterial infections.** *Nat Rev*  
2 *Microbiol* 2015.
- 3 50. Bennett WP, Hollstein MC, Hsu IC, Sidransky D, Lane DP, Vogelstein B, Harris  
4 CC: **Mutational spectra and immunohistochemical analyses of p53 in**  
5 **human cancers.** *Chest* 1992, **101**:19S-20S.
- 6 51. Hagiwara N, Mechanic LE, Trivers GE, Cawley HL, Taga M, Bowman ED,  
7 Kumamoto K, He P, Bernard M, Doja S, et al: **Quantitative detection of p53**  
8 **mutations in plasma DNA from tobacco smokers.** *Cancer Res* 2006,  
9 **66**:8309-8317.
- 10 52. Wu S, Rhee KJ, Albesiano E, Rabizadeh S, Wu X, Yen HR, Huso DL, Brancati  
11 FL, Wick E, McAllister F, et al: **A human colonic commensal promotes colon**  
12 **tumorigenesis via activation of T helper type 17 T cell responses.** *Nat Med*  
13 2009, **15**:1016-1022.
- 14 53. Zhu L, Jing S, Wang B, Wu K, Shenglin MA, Zhang S: **Anti-PD-1/PD-L1**  
15 **Therapy as a Promising Option for Non-Small Cell Lung Cancer: a Single**  
16 **arm Meta-Analysis.** *Pathol Oncol Res* 2016, **22**:331-339.
- 17 54. Sivan A, Corrales L, Hubert N, Williams JB, Aquino-Michaels K, Earley ZM,  
18 Benyamin FW, Lei YM, Jabri B, Alegre ML, et al: **Commensal Bifidobacterium**  
19 **promotes antitumor immunity and facilitates anti-PD-L1 efficacy.** *Science*  
20 2015, **350**:1084-1089.
- 21 55. Tartour E, Zitvogel L: **Lung cancer: potential targets for immunotherapy.**  
22 *Lancet Respir Med* 2013, **1**:551-563.
- 23 56. Zhang C, Cleveland K, Schnoll-Sussman F, McClure B, Bigg M, Thakkar P,  
24 Schultz N, Shah MA, Betel D: **Identification of low abundance microbiome in**  
25 **clinical samples using whole genome sequencing.** *Genome Biol* 2015,  
26 **16**:265.
- 27 57. Zheng YL, Loffredo CA, Alberg AJ, Yu Z, Jones RT, Perlmutter D, Enewold L,  
28 Krasna MJ, Yung R, Shields PG, Harris CC: **Less efficient g2-m checkpoint is**  
29 **associated with an increased risk of lung cancer in African Americans.**  
30 *Cancer Res* 2005, **65**:9566-9573.
- 31 58. Kozich JJ, Westcott SL, Baxter NT, Highlander SK, Schloss PD: **Development**  
32 **of a Dual-Index Sequencing Strategy and Curation Pipeline for Analyzing**  
33 **Amplicon Sequence Data on the MiSeq Illumina Sequencing Platform.**  
34 *Applied and Environmental Microbiology* 2013, **79**:5112-5120.
- 35 59. Caporaso JG, Kuczynski J, Stombaugh J, Bittinger K, Bushman FD, Costello EK,  
36 Fierer N, Pena AG, Goodrich JK, Gordon JI, et al: **QIIME allows analysis of**  
37 **high-throughput community sequencing data.** *Nat Methods* 2010, **7**:335-336.

38

39

40

41

1 **Figure Legends:**

2 **Figure 1.** The bacterial profile and diversity of the lung microbiome in non-diseased and  
3 cancerous tissues. A) 16S rRNA gene sequences from non-diseased lung (ImA or HB;  
4 top), non-tumor adjacent (NT) and tumor (T) assigned to OTUs or proportional  
5 abundance of metatranscriptomic sequences (TCGA; bottom) at the phylum level  
6 showing the most dominant taxa for each tissue type. B) Alpha diversity between non-  
7 diseased lung tissue (ImA and HB) non-tumor adjacent (NT) and tumors from 16S rRNA  
8 gene sequencing using Chao1 (richness) or inverse Simpson index.  $^*(P<0.05)$ ,  
9  $^{**}(P<0.01)$ . Test of significance is Mann-Whitney. ImA - immediate autopsy; HB –  
10 hospital biopsy.

11 **Figure 2.** Taxonomic consortia differentiating smoking status and histological subtype of  
12 lung cancer. A) Heat maps showing top differentially abundant genera (NCI-MD) (Mann-  
13 Whitney  $p$ -value $<0.05$ ; \* overlapping between NCI-MD and TCGA) between AD and  
14 SCC lung cancer tissue sorted by histological subtype and smoking status. B) Heat map  
15 showing genera (TCGA) that that are differentially abundant between AD and SCC  
16 (Mann-Whitney FDR corrected  $P<0.05$ ), sorted by histological subtype and smoking. C)  
17 Forest plot of odds ratios for genera in NCI-MD data set that are significantly associated  
18 with SCC compared to AD in tumors (adjusted odds ratio  $P<0.05$ ). D) Forest plot of  
19 odds ratios for species in TCGA data set that are significantly associated with SCC  
20 versus AD in tumors (adjusted odds ratio FDR corrected  $P<0.05$ ).

21 **Figure 3.** Relative abundance of *Acidovorax* stratified by smoking status and  
22 histological subtype. A) Relative abundance of *Acidovorax* stratified by smoking status  
23 in NCI-MD (Left) and TCGA (Right) data sets. B) Relative abundance of *Acidovorax* in

1 Never, Former and Current smokers stratified by histological subtype in the NCI-MD  
2 (Left) and TCGA (Right) data sets. C) Representative FISH images of tumor tissue  
3 sections using fluorescent probe specific to *Acidovorax*. D) Quantification of *Acidovorax*  
4 probe reactivity (10 fields; at least 300 cells counted) showing percentage (%) of cells  
5 with perinuclear probe reactivity from two lung cancer cases (15713 – SCC/current  
6 smoker; 20172 – SCC/former smoker). \*( $P < 0.05$ ), \*\*( $P < 0.01$ ), \*\*\*\*( $P < 0.0001$ ). Test of  
7 significance are Mann-Whitney or Kruskal-Wallis and Dunn's multiple comparisons test.  
8 NS = non-significant.

9 **Figure 4.** Mutations in *TP53* associated with abundance of taxonomic signature specific  
10 to squamous cell lung tumors. A) Heat map of genus-level abundance in NCI-MD data  
11 colored by mutation status, *TP53* wild type or mutated, smoking and histological  
12 subtype in all lung tumor samples. B) Heat map of genus-level abundance from TCGA  
13 data in all tumors colored by mutation status, *TP53* wild type or mutated, smoking and  
14 histological subtype. C-D) Fold change in mean abundance of SCC-associated taxa in  
15 NCI-MD or TCGA tissues comparing *TP53* mutated to wild type. Tests of significance  
16 are Mann-Whitney. Fold change among all taxa in D) are significant after FDR  
17 correction  $< 0.01$ . (NCI-MD;  $SCC_{wt}=11$ ,  $SCC_{mut}=35$  and TCGA;  $SCC_{wt}=59$ ,  $SCC_{mut}=118$ )

18

19

20

21

22

23

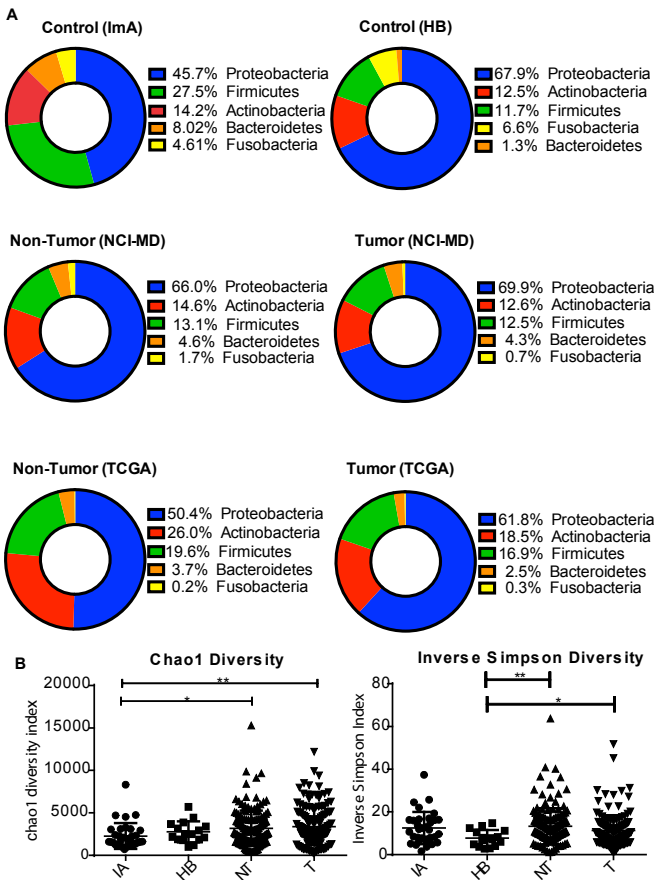
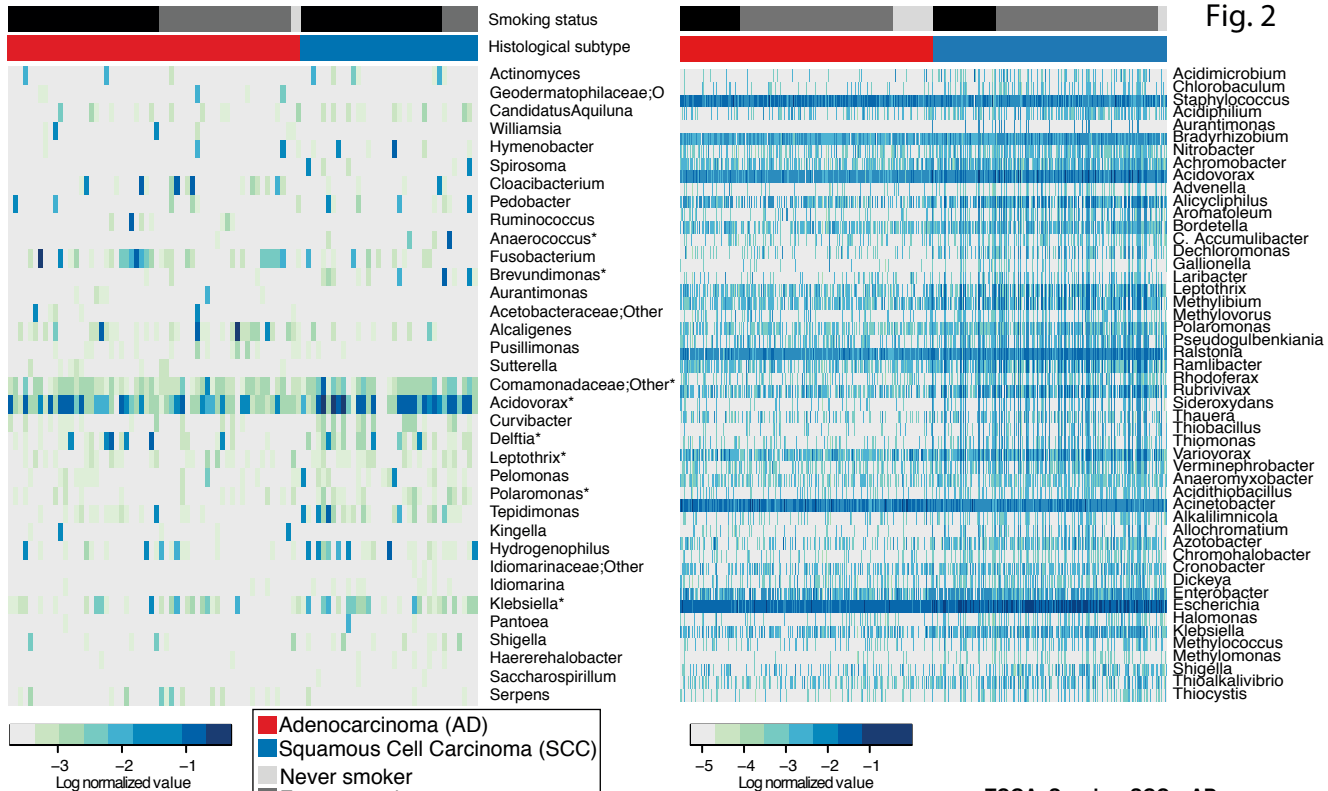
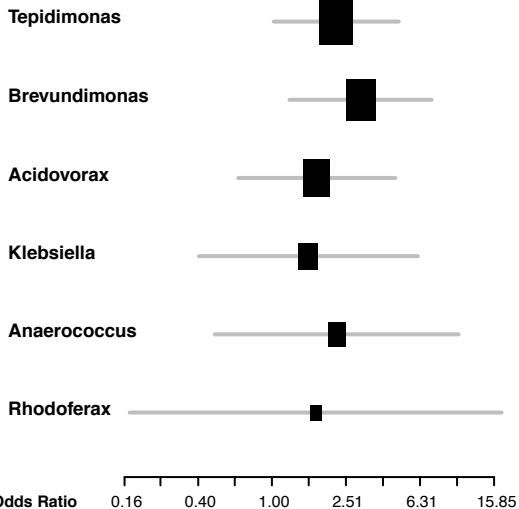


Fig. 1



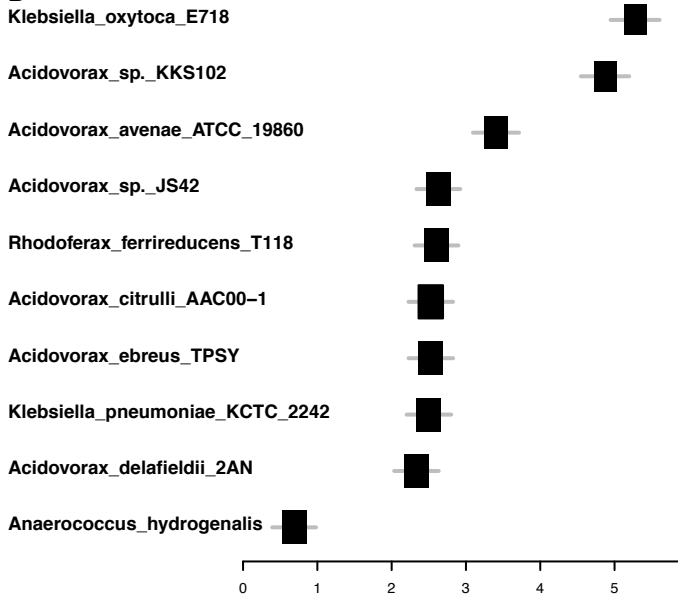
C

NCI-MD -Genus: SCC v AD



D

TCGA -Species: SCC v AD



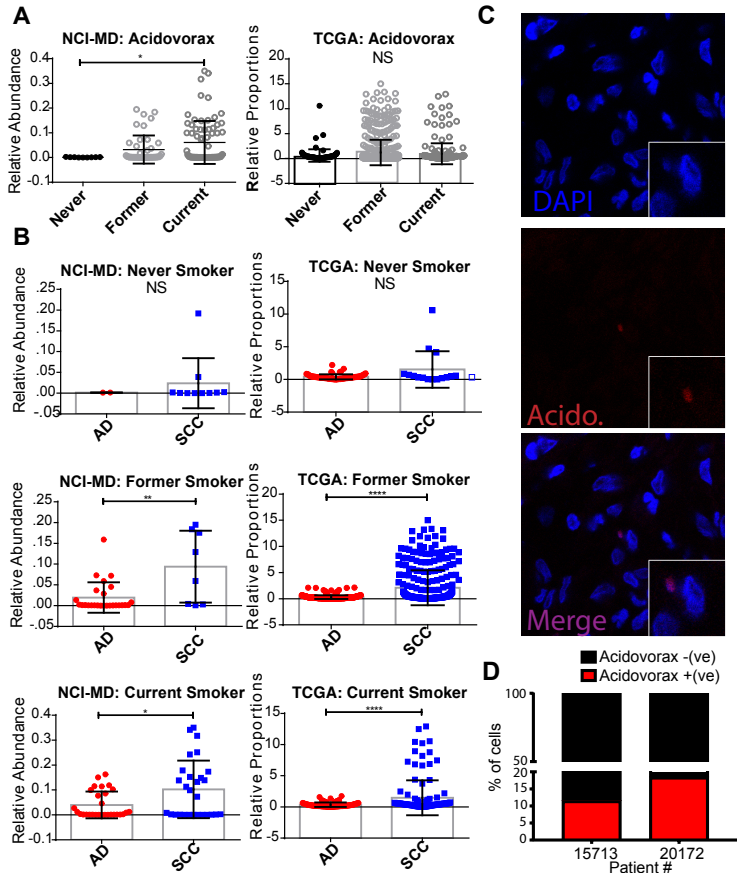


Fig. 3

**Fig. 4**

